Appl Nanosci (2014) 4:379–383
DOI 10.1007/s13204-013-0207-z

ORIGINAL ARTICLE

Solvothermal growth of $Ti_{1-x}Sn_xO_2$ semiconductor nanopowders

Mohamed M. Rashad · Osama A. Fouad

Received: 1 February 2013 / Accepted: 25 February 2013 / Published online: 29 March 2013

Abstract $Ti_{1-x}Sn_xO_2$ nanoparticles have been successfully prepared by solvothermal method. Sn (II) chloride dihydrate powder and Ti (IV) chloride liquid were used as Sn and Ti precursors in HCl/HNO_3 acid mixture. SEM and EDX analyses showed that the precipitated powders are composed mainly of Ti, Sn and O elements. While the sample treated at 100 °C showed high-intensity chlorine EDX peak, the one treated at 150 °C did not. XRD patterns showed that precipitated powder at 150 °C for different reaction time intervals (6–48 h) were in the form of rutile crystallographic structure. Calculated crystallite size (~1.30 nm) using Scherrer's formula and Williamson–Hall plot showed that the micro strain effect was very low. UV–Vis spectrometry showed that two absorption peaks could be detected at 3.86 and 3.62 eV, respectively. The obtained results can open the door toward synthesis of other nanocomposite semiconductors at low temperatures without the need of further annealing and with unique properties.

Keywords Coupled semiconducting oxides · TiO_2–SnO_2 · Nanostructures · Optical properties

Introduction

The tailoring and designing of nanocomposites powders and thin films based on semiconducting oxide materials are important objectives for advanced industrial applications (Beltrán et al. 2008; Chou and Wang 2006; Aprile et al. 2008; Zakrzewska 2001; Santen and Neurock 2006). Mixed oxide compounds, such as solid solutions of ZnO–SnO_2, WO_3–TiO_2, SnO_2–WO_3 and SnO_2–TiO_2, seem to be promising candidates for various technological applications. Such complex oxide systems may benefit from the combination of the best physical and chemical properties of the pure compounds (Chou and Wang 2006; Aprile et al. 2008; Zakrzewska 2001; Santen and Neurock 2006).

Among all, mixed semiconducting oxide systems based on both ceramic TiO_2 and SnO_2 material with rutile structure are an attractive group of materials in terms of the electronic, optical properties, thermal and chemical stabilities (Beltrán et al. 2008; Santen and Neurock 2006). TiO_2 is an n-type wide band gap (E_g ~3.0 to 3.2 eV) semiconductor that has been extensively studied by many research groups in the last decade (Nho and Cuong 2008). It has been widely employed in many photocatalytic applications for pollutants decomposition and in photo electrochemical solar cell fabrication (Hamoon et al. 2011). On the other hand, SnO_2 is an n-type wide band gap semiconductor (E_g ~3.6 eV) that has several interesting properties which have made it a reliable material for catalytic and gas sensing applications.

TiO_2 and SnO_2 nanopowders and thin films are prepared by various synthesis techniques (Beltrán et al. 2008; Shang et al. 2004; Bueno and Varela 2006). Hydrothermal (water medium) or solvothermal (solvent medium) method is an outstanding route of synthesis of narrow size distribution nanoparticles and low particle agglomeration nanostructures with high purity. They are usually carried out in a sealed vessel (bomb, autoclave, etc.) where water or solvents are brought to temperatures above their boiling points by increasing the pressures resulting from heating. Unlike the cases of co-precipitation and sol–gel methods, the

M. M. Rashad · O. A. Fouad (✉)
Central Metallurgical Research and Development Institute, CMRDI, P.O. Box 87, Helwan 11421, Cairo, Egypt
e-mail: oafouad@yahoo.com

products of hydrothermal reactions are usually crystalline and in most cases do not require post annealing treatments.

Here in we report on the results obtained from the synthesis and characterization of TiO_2–SnO_2 nanoparticles using the solvothermal method. The factors affecting the synthesis process were investigated. The produced materials were also characterized by studying the chemical composition, morphological structure and optical properties.

Experimental

Materials

Tin (II) chloride dihydrate powder ($SnCl_2{\cdot}2H_2O$, 98 %, Sigma-Aldrich) and titanium (IV) tetrachloride liquid ($TiCl_4$, 99 %, Sigma-Aldrich) were used as tin and titanium precursors. Hydrochloric (HCl, 35 %, Adwic) and nitric acids (HNO_3, 65 %, Adwic) were used as dissolving and oxidizing agents for stannous chloride. Ammonia solution (NH_4OH, 25 %, Adwic) was used as a base. Bi-distilled water was used for making solutions, dilution and washing the products. All chemicals were used in this study were of pure grade and used without any further treatment.

Synthesis process

The solvothermal synthesis process was carried out in a Teflon-lined stainless steel autoclave. A clear solution was obtained through mixing of proper amounts of tin chloride and titanium tetrachloride. The pH of the solution was adjusted to 7 by adding ammonia solution dropwisely. The mixture was then introduced into the autoclave and subjected to heat treatment at 100–200 °C for 6–48 h. Then the cooled precipitates were filtered, washed with distilled water, dried and kept for further investigations.

Characterization of the prepared powders

White precipitates were obtained after completing the course of the reaction. Morphologies and chemical compositions of the precipitated powders were investigated by scanning electron microscope (SEM; Jeol JSM-5410, Japan). EDX analysis was performed to study the chemical composition of the precipitated powders. Crystal structure and phase identification of the precipitated powders were performed at room temperature by X-ray diffraction (XRD; Bruker axs D8, Germany) with Cu–K_α ($\lambda = 1.5418$ Å) radiation and secondary monochromator in the 2θ range from 20° to 80°. Crystallite size was calculated using Scherrer's formula. Micro strain broadening was also investigated using Williamson–Hall's plot. UV–Vis spectrum was recorded at room temperature in the wavelength range from 200 to 900 nm using a spectrophotometer (UV–Vis, JASCO *V-570*, Japan).

Results and discussion

Microstructure and composition

Figure 1a, b shows the SEM images and EDX analyses of the samples prepared at 100 and 150 °C for 6 h, respectively. It is clear that the samples are composed mainly of compact and nonporous structures. The materials after centrifuging and drying look like multilayers stacks composed of interconnected nanoparticles. The nanoparticles show high degree of agglomeration. This might be due to acidic solutions nature during synthesis. EDX analyses showed that both samples are composed mainly of titanium, tin and oxygen. However, the sample processed at 100 °C shows the presence of appreciable amount of elemental Cl which is characterized by high-intensity peak (Fig. 1c). The presence of such amount of Cl might be due to incomplete reaction at 100 °C. In contrary to this, the sample solvothermally treated at 150 °C does not show any EDX peak for Cl (Fig. 1d). This indicates that the reaction at 150 °C is completed. The weight and atomic percentage of the elements derived from the EDX data are summarized in Table 1. The calculated $x = \text{Sn/Sn} + \text{Ti}$ atomic ratios for samples prepared at 100 and 150 °C are 0.47 and 0.43, respectively.

Crystal structure and phase identification

Figure 2 shows the XRD patterns of the as-prepared TiO_2–SnO_2 samples at 150 °C, for different time intervals from 6 to 48 h. The diffraction stick patterns of titanium tin oxide phase (JCPDS card # 01-07-4411), rutile (TiO_2, JCPDS card # 75-1753) and cassiterite (SnO_2, JCPDS card # 77-0450) are also shown there for comparison. It is clear that the prepared samples have polycrystalline rutile structure. Generally, the diffraction peaks are broad with noticeable low intensities. The main diffraction peaks from the crystallographic planes (110), (101), (200) and (211) of rutile structure are comprised between the lines corresponding to SnO_2 and TiO_2 phases. There is a slight shift in the peak positions toward higher diffraction angels upon increasing the reaction time intervals. This shift might be due to the progression of the lattice parameters from those of SnO_2 to those of TiO_2 as the reaction proceeded. This result is in agreement to that obtained from EDX analysis. This means that more SnO_2 are involved in the reaction which is indicated by the increase in the interplanar d_{hkl} spacing, since Sn^{4+} has larger ionic radius (0.071 nm) than that of Ti^{4+} (0.068 nm) (Naidu and Virkar 1998).

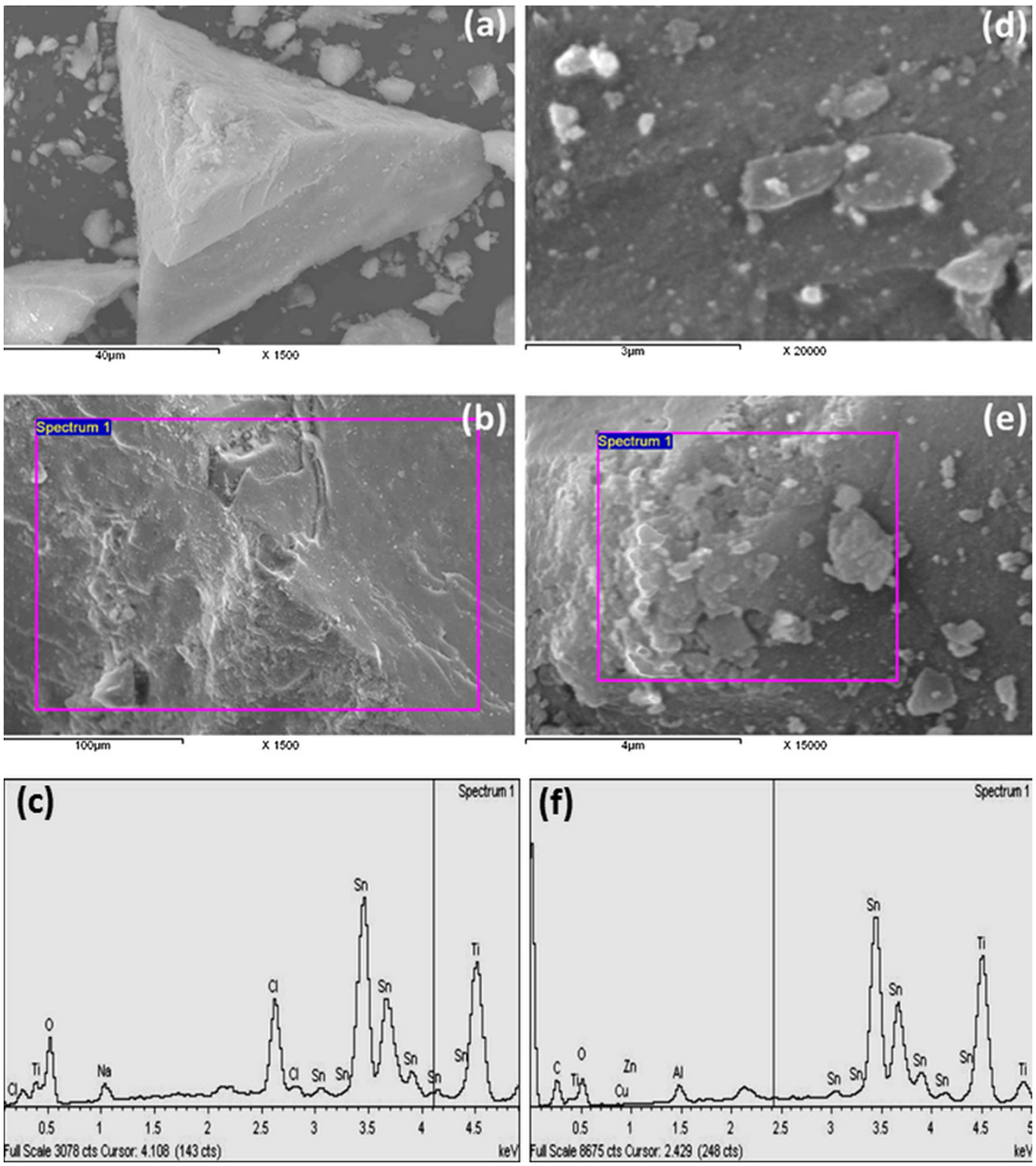

Fig. 1 SEM images and EDX analyses of the as-prepared TiO_2–SnO_2 samples solvothermally treated at various reaction temperatures **a**, **b** 100 °C, **c** corresponding EDX analysis, **d**, **e** 150 °C and **f** corresponding EDX analysis

The crystallite size (Cs) of the prepared material has been evaluated by Scherrer's formula:

$$\mathrm{Cs} = k\lambda/\beta\cos\,\theta \qquad (1)$$

where k is a correction factor taken as 0.94, λ is wavelength of Cu target-K_α X-ray radiations (0.15418 nm) used, β is broadening of diffraction line measured at half of its maximum intensity (FWHM in radian), and θ is Bragg's diffraction angle (in degree). The crystallite size of the prepared $Ti_{1-x}Sn_xO_2$ nanoparticles calculated based on the highest intensity diffraction plane (110) has been found to be 1.30 nm. The crystallite size as a function of reaction time intervals is represented in Fig. 3. Crystallite size can be affected by the micro strain which may lead to a systematic shift of atoms due to poor crystallinity, point defects or plastic deformation that cause peak broadening.

Combining Scherrer's formula (broadening due to crystallite size) together with strain (broadening due to strain) effect, we can get the following formula:

Table 1 Weight and atomic percentage of the elements composing the prepared samples

Element	Weight (%)		Atomic (%)	
	Sample at 100 °C	Sample at 150 °C	Sample at 100 °C	Sample at 150 °C
Ti	12.62	16.64	6.63	8.79
Sn	28.06	31.69	5.96	6.75
O	50.83	31.74	80.02	50.18
Cl	4.96	–	3.52	–

$$\beta_{str} = 4\varepsilon \tan\theta \quad (2)$$

The total broadening β_{total} equals:

$$\beta_{total} = \beta_c + \beta_{str} \quad (3)$$

where β_c is the broadening due to crystallite size and β_{str} broadening due to strain.

Then β_{total} can be expressed as:

$$\beta_{total}\cos\theta = k\lambda/Cs + 4\varepsilon \sin\theta \quad (4)$$

By plotting β_{total} cos θ versus sin θ, we can get Williamson–Hall straight line (inset in Fig. 3), where the slope will be the gradient 4ε and the intercept will be $k\lambda$/Cs from which crystallite size can be calculated. The crystallite size (Cs) is found to be 1.35 nm. This value

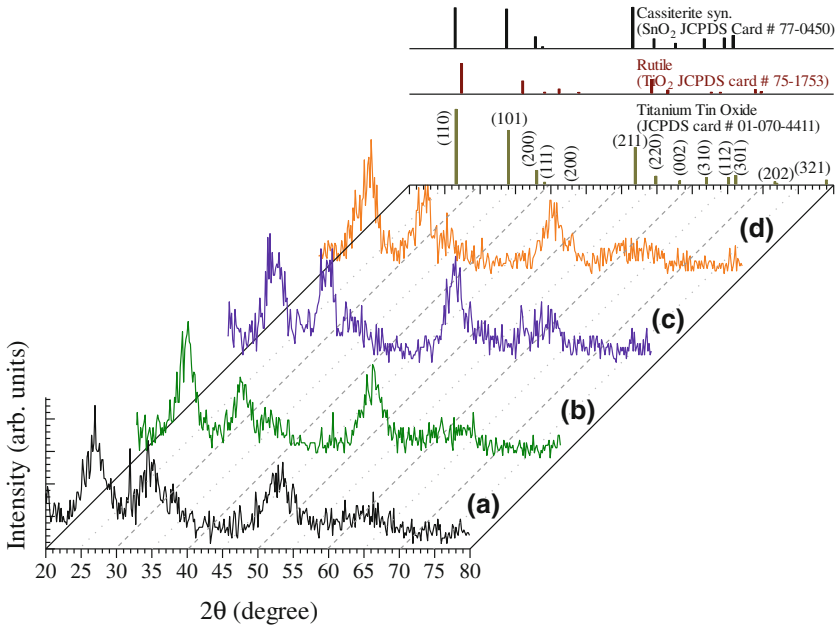

Fig. 2 XRD patterns of the as-prepared TiO_2–SnO_2 samples at 150 °C, for different time intervals *a* 6 h, *b* 12 h, *c* 24 h and *d* 48 h. The diffraction stick pattern of titanium tin oxide phase is also shown for comparison

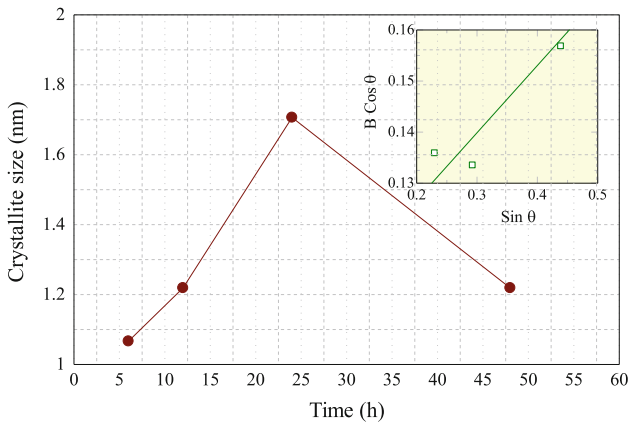

Fig. 3 Crystallite size of the precipitated TiO_2–SnO_2 powder as a function of reaction time. The *inset* is the Williamson–Hall plot

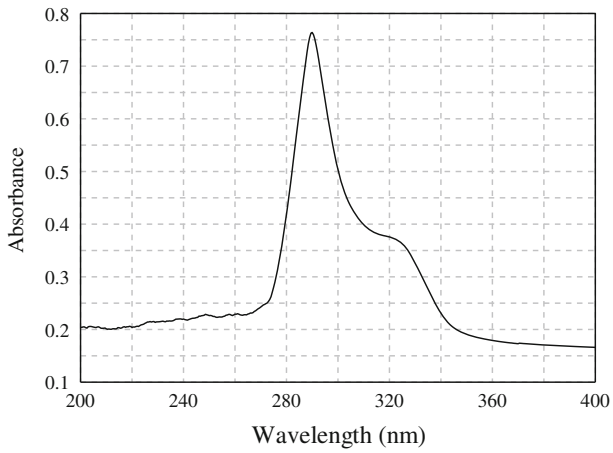

Fig. 4 UV–Vis spectrum of the precipitated powder at 150 °C reaction temperature for 6 h reaction time

reflects that broadening resulting from micro strain effect is very low.

Optical properties

Figure 4 depicts the normalized absorbance UV–Vis absorption spectrum of the sample prepared at 150 °C for 6 h. The absorption peak is most likely splitted into two absorption bands. The absorption edge and band gap energies can be detected and calculated from the spectrum data. The absorption edge for the first peak is determined to be 321 nm. This is corresponding to a band gap of 3.86 eV. The other peak is detected at 342 nm which is corresponding to the band gap energy of 3.62 eV. The sample shows blue shift toward higher energy gap from that of single TiO_2 and SnO_2.

Conclusions

Nanocomposite coupled semiconducting powders based on TiO_2–SnO_2 have been synthesized successfully. Tin (II) chloride dihydrate powder and titanium (IV) chloride liquid were used as Sn and Ti precursors in HCl/HNO_3 acid mixture at reaction temperature of 100–200 °C for reaction time intervals of 6–48 h. The sample prepared at 100 °C showed incompletion of the reaction, since intense chlorine EDX peaks are detected. Calculated crystallite size was in the range of $\sim$1.30 to 1.35 nm using Scherrer's formula and Williamson–Hall plot. UV–Vis spectrum showed that two absorption peaks could be detected at 3.86 and 3.62 eV, respectively. The obtained results can open the door toward synthesis of other coupled semiconductors at low temperatures without the need of further annealing and with unique properties.

References

Aprile C, Corma A, Garcia H (2008) Enhancement of the photocatalytic activity of TiO_2 through spatial structuring and particle sizencontrol: from subnanometric to submillimetric length scale. Phys Chem Chem Phys 10:769

Beltrán A, Andrés J, Sambrano JR, Longo E (2008) Density functional theory study on the structural and electronic properties of low index rutile surfaces for $TiO_2/SnO_2/TiO_2$ and $SnO_2/TiO_2/SnO_2$ composite systems. J Phys Chem A 112:8943

Bueno PR, Varela JA (2006) Electronic ceramics based on polycrystalline SnO_2, TiO_2 and $(Sn_xTi_{1-x})O_2$ solid solution. Mat Res 9:371

He JH, Wu TH, Hsin CL, Li KM, Chen LJ, Chueh YL, Chou LJ, Wang ZL (2006) Beaklike SnO_2 nanorods with strong photoluminescent and field-emission properties. Small 2:116

Hamoon HZR, Devi GS, Beigi H, Rao JVR, Reddy KR, Nanaji A (2011) Synthesis and characterization of Co-doped SnO_2/TiO_2 semiconductor nano crystallites via sol-gel method. J Nano-Electron Phys 3:59

Naidu HP, Virkar AV (1998) Low-temperature TiO_2–SnO_2 phase diagram using the molten-salt method. J Am Ceram Soc 81:2176

Nho PV, Cuong TK (2008) Preparation and characterization of nanocomposite TiO_2/SnO_2 films. VNU J Sci Math Phys 24:42

Santen RA, Neurock M (2006) Molecular heterogeneous catalysis (a conceptual and computational approach). Wiley, Weinheim

Shang J, Yao W, Zhua Y, Wu N (2004) Structure and photocatalytic performances of glass/SnO_2/TiO_2 interface composite film. Appl Catal A 257:25

Zakrzewska K (2001) Mixed oxides as gas sensors. Thin Solid Films 391:229